
**Liquid Crystals**
Publication details, including instructions for authors and subscription information:
http://www.informaworld.com/smpp/title~content=t713926090

# Experimental study of the growth of cholesteric fingers subjected to an AC electric field and a temperature gradient

P. Oswald[a]
[a] University of Lyon, Physics Laboratory, Ecole Normale Supérieure de Lyon, 46 Allée d'Italie, 69364 Lyon, Cedex 07, France

**To cite this Article** Oswald, P.(2009) 'Experimental study of the growth of cholesteric fingers subjected to an AC electric field and a temperature gradient', Liquid Crystals, 36: 9, 967 — 975
**To link to this Article: DOI:** 10.1080/02678290903165508
**URL:** http://dx.doi.org/10.1080/02678290903165508

*Liquid Crystals,*
Vol. 36, No. 9, September 2009, 967–975

Taylor & Francis
Taylor & Francis Group

# Experimental study of the growth of cholesteric fingers subjected to an AC electric field and a temperature gradient

P. Oswald*

*University of Lyon, Physics Laboratory, Ecole Normale Supérieure de Lyon, 46 Allée d'Italie, 69364 Lyon, Cedex 07, France*

*(Received 26 June 2009; final form 6 July 2009)*

We study the behaviour of cholesteric fingers of the first and second types (CF1 and CF2, respectively) which form in cholesteric samples treated for homeotropic anchoring when they are subjected to the combined action of an AC electric field and a temperature gradient. We investigate under which conditions each type of finger can drift and form a spiral. We then show that the ends of the growing CF1 follow circular trajectories, the curvatures of which depend linearly on the temperature gradient. This observation opens the possibility of measuring the thermal Lehmann coefficient in any cholesteric liquid crystal at all temperatures.

**Keywords:** liquid crystals; cholesteric fingers; spiral; circular growth; Lehmann effect



## 1. Introduction

Cholesteric fingers have been known for a long time (for a review, see (*1,2*)). They form in samples treated for homeotropic anchoring when the cholesteric pitch is comparable to the sample thickness. Under this condition, the fingers are isolated and coexist with the homeotropic nematic phase (unwound cholesteric). They can be of four different types (at least, see (*3*)), but the most common, on which we focus in this paper, are the cholesteric fingers of the first and second types (CF1 and CF2, respectively). The CF1, the structure of which was described for the first time by Press and Arrott (*4*), are continuous everywhere, whereas the CF2, discovered by Gil and Gilli (*5*), contain point defects in their two ends (*6*). Their structures, recalled in Figure 1, are now well known and have been recently confirmed by direct observation using fluorescence confocal polarised microscopy (*7*).

It turns out that when the sample thickness $d$ is larger than the equilibrium pitch $p$, the fingers are no longer isolated but form a periodic pattern. Under this condition and if the liquid crystal has a positive dielectric anisotropy, one way to recover isolated fingers is to impose an AC electric field which tends to unwind the helical structure of the phase. More precisely, there exists for each confinement ratio $C = d/p$ a voltage $V_2$ (or, equivalently, an electric field $E_2 = V_2/d$) at which the fingers coexist with the nematic phase. If the applied voltage $V$ is smaller than $V_2$, the fingers lengthen from their two ends, whereas they shorten if the voltage is larger than $V_2$.

In this paper, we study the dynamical behaviour of the CF1 and CF2 when the sample is subjected to the combined action of an electric field close to $E_2$ and a temperature gradient $G$ perpendicular to the glass plates. The goal of this experiment is to find a general method for measuring the thermal Lehmann coefficient at all temperatures in any cholesteric liquid crystal. We recall that, for practical reasons, this coefficient has so far only been measured at the clearing temperature of the cholesteric phase (when it coexists with its isotropic liquid) (*8,9*) and close to the compensation temperature (at which the pitch diverges) of some special mixtures (*10–13*).

The plan of the article is as follows. In Section 2, we present the experiment. In Section 3, we give the phase diagram for the CF1. In Section 4, we study under which conditions the CF1 and the CF2 drift perpendicularly to their axes and form spirals. In Section 5, we study the circular growth of the CF1 when the electric field is smaller than $E_2$. We show that this phenomenon is induced by the temperature gradient and could be used for measuring the thermomechanical Lehmann coefficient. Finally, we draw conclusions in Section 6.

## 2. Experiment

Our experiment consists of observing the growth of cholesteric fingers which form in homeotropic samples subjected to the combined action of an AC electric field and a temperature gradient perpendicular to the glass plates. The liquid crystal chosen was an eutectic mixture of 8CB (4-n-octyl-4′ cyanobiphenyl from Frinton Laboratories, Inc.) and 8OCB (4-n-octyloxy-4′ cyanobiphenyl

*Email: patrick.oswald@ens-lyon.fr

ISSN 0267-8292 print/ISSN 1366-5855 online

DOI: 10.1080/02678290903165508
http://www.informaworld.com

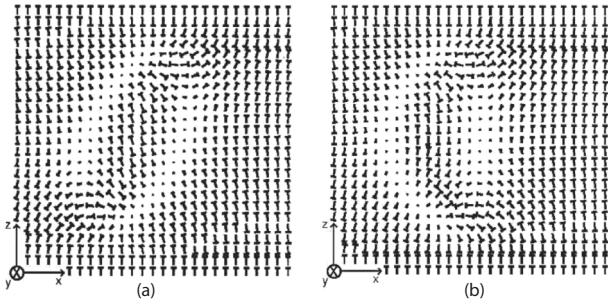


Figure 1. (a) Director field inside a finger of the first type. The nail representation is used in order to show that the director $\boldsymbol{n}$ is tilted with respect to the ($x$, $z$) plane perpendicular to the finger axis. (b) Director field inside a finger of the second type. As $\boldsymbol{n} \Leftrightarrow -\boldsymbol{n}$, a CF1 is invariant under a $\pi$ rotation around the finger axis (parallel to the $y$-axis), whereas a CF2 is not.

(from Synton Chemicals GmbH & Co.) in the mass proportion of 57:43 (see (*14*)) doped with 1.14 wt% of the chiral molecule R811 (from Merck Ltd). This mixture exhibits the following phase transitions (*9*):

$$\text{Smectic } A \overset{45.5^\circ\text{C}}{\rightarrow} \text{Cholesteric} \overset{54.4-55.2^\circ\text{C}}{\rightarrow} \text{Isotropic liquid.}$$

The liquid crystal is embedded between two parallel transparent electrodes (glass plates with an ITO layer). The surfaces of the electrodes are treated for strong homeotropic anchoring by spin-coating a thin layer of polyimide 0626 from Nissan (diluted to 3% in weight in solvent 26 from Nissan). The latter is dried for one hour at 80°C and is then polymerised for two hours at 160°C. The sample is sandwiched between two transparent ovens which are separately regulated in temperature thanks to two circulating baths (for a description of the setup, see (*8*)). Two 60 μm-thick layers of a glycerol–water mixture ensure a good thermal contact between the sample and the two ovens. In this way, it is possible to impose a well-controlled temperature gradient to the sample. In the following, we denote by $\Delta T = T_b - T_t$ the temperature difference between the bottom and top ovens, by $T = (T_b + T_t)/2$ the average temperature of the sample and by $G$ the temperature gradient. Previous calibration has shown that $G(^\circ\text{C } mm^{-1}) \approx 1.5\ \Delta T\ (^\circ\text{C})$ (see (*8*)). The sinusoidal electric field was produced using a HP 3325B function generator. The charge relaxation frequency $f_c$ of the samples was measured with a HP 4284A precision LCR meter. We found that in all samples $f_c \approx$ 500–600 Hz.

## 3. Phase diagram

The phase diagram of the CF1 is shown in Figure 2(a) for a 15 μm-thick sample. There is no temperature gradient imposed to the sample ($G = 0$). In the abscissa is the temperature and in the ordinate is the root mean square (r.m.s.) voltage between the electrodes. The measurements are performed under a sinusoidal AC field at 1 kHz. Four lines are visible. Lines $V_0$ and $V_3$ correspond to the spinodals of the nematic and the fingers, respectively. Line $V_2$ marks the limit of coexistence between the CF1 and the nematic. Finally, $V_1$ gives the limit of stability of the growing CF1 with respect to the splitting of their rounded ends. We note that all of these voltages tend to zero when the temperature approaches the cholesteric-to-smectic A phase transition temperature. This behaviour is due to both the divergence of the cholesteric pitch and the increase of the ratio $K_3/K_2$ of the bend constant over the twist constant at the transition.

We also measured these voltages as a function of the sample thickness at temperature $T$ = 48°C and frequency $f$ = 1 kHz. As we can see in Figure 2(b),

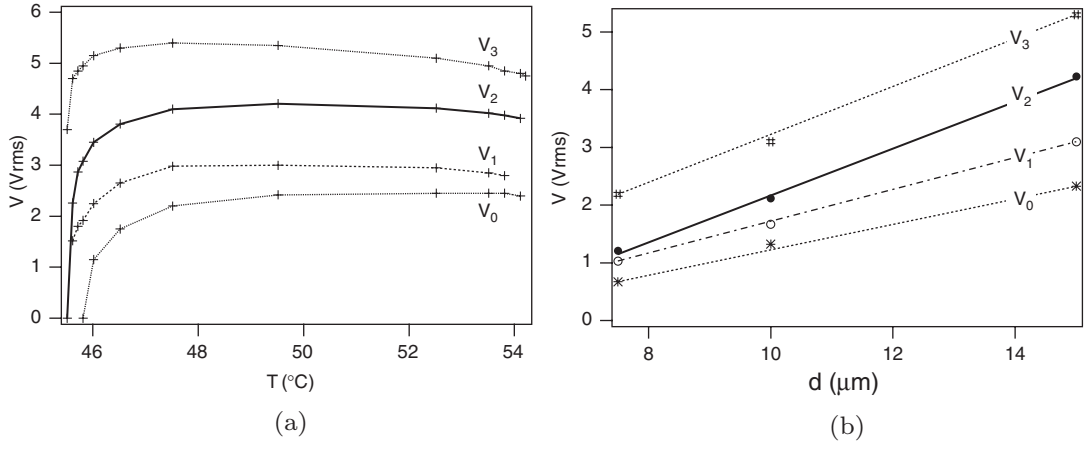


Figure 2. (a) Phase diagram measured in a 15 μm-thick sample as a function of temperature at $f$ = 1 kHz and $G$ = 0. (b) Phase diagram measured at $T$ = 48°C as a function of the sample thickness at $f$ = 1 kHz and $G$ = 0.

they are linear functions of the thickness in the investigated range of thicknesses (between 7.5 and 15 μm).

## 4. Spirals

Spirals form spontaneously when the fingers drift perpendicularly to their axes. The drift can be induced by the electric field (*15–22*) or by the temperature gradient (*23*). We observed three different types of spiral. We describe them successively, starting with the most frequently observed.

### *4.1 CF2 spirals driven by the electric field*

CF2 spirals occur spontaneously in all samples at low frequency, in the conducting regime ($f < f_c$), whatever the temperature and the temperature gradient, when the applied voltage is equal or a bit larger than $V_2$. CF2 are easily recognisable by increasing the voltage just above $V_3$: while the CF1 break spontaneously and collapse, the CF2 remain stable and shorten from their two ends until forming a spherulite (*6,19*). An example of a CF2 spiral is shown in Figure 3.

In the following we denote by $v_{CF2}$ the drift velocity of the finger far from the spiral centre. As we can see in Figure 4(a), this quantity decreases exponentially with frequency with a cutoff frequency $f_{CF2} \sim 1.5 f_c$. This frequency behaviour has already been observed (*20*) and has been explained theoretically by Tarasov *et al.* (*22*) as being due to electrohydrodynamic effects induced by Carr–Helfrich charge separation. In addition, we observed that $v_{CF2}$ depends little on the temperature except close to the smectic A phase where it strongly decreases (Figure 4(b)). This decrease is certainly due to the increase of the rotational viscosity $\gamma_1$ when the smectic phase is approached (*24, 25*). Finally, we emphasise that we did not observe any significant drift of the CF2 in the dielectric regime due to the temperature gradient. We return to this point later.

Figure 3. CF2 spiral observed between crossed polarisers. The white scale bar is 100 μm long. Here $d = 15$ μm, $\Delta T = 40°C$, $T = 50°C$, $V = 4.5\,V_{rms}$ and $f = 100$ Hz.

### *4.2 CF1 spirals driven by the electric field*

By increasing the temperature, it is possible to melt partly the cholesteric phase in the temperature gradient. The experiment was performed with a 15 μm-thick sample under a temperature gradient $\Delta T = 40°C$. We observed that between 54.1 and 54.4°C, the cholesteric phase melts into droplets close to the hot plate. In this temperature interval, droplets are stable as they are observed regardless of the way the final temperature has been reached (by heating or cooling). Fingers also form but they are strongly deformed by the droplets and they look fuzzy under the microscope. By contrast, it becomes possible to stabilise a thin layer of isotropic liquid in contact with the cholesteric phase above 54.4°C, when it is thicker than 2–3 μm. This new configuration is easily obtained by first melting the sample almost completely and then decreasing the temperature slowly (droplets are indeed difficult to eliminate by just heating). The sample then consists of a layer of cholesteric phase in contact with the cold plate superimposed to a layer of isotropic liquid in contact with the hot plate. Between 54.4 and 55°C, fingers still form in the cholesteric layer whereas they disappear (unwinding transition) above 55°C when the cholesteric layer becomes too thin. Finally, the sample is completely melted above 55.5°C. We estimated that at 54.4°C the cholesteric layer is about 13 μm thick while at 55°C its thickness must be close to the equilibrium cholesteric pitch, of the order of 5 μm at the transition (*9*).

In the following, we focus on fingers which form between 54.4 and 55°C in the cholesteric layer in contact with the isotropic liquid. These fingers are very similar to those observed before melting although the anchoring is not homeotropic at the nematic–isotropic interface (the tilt angles of the molecules with respect to the normal to the interface of the order of 50° have been found in cyanobiphenyls (*26*) at the nematic–isotropic interface). There still exists a voltage $V_2$ at which the fingers coexist with the nematic phase. At this voltage, the nematic is dark between crossed polarisers, which shows that the tilted anchoring of the molecules at the interface with the isotropic liquid is broken and becomes homeotropic. We also observed that all fingers form segments with a pointed tip and a rounded tip, which spontaneously collapse above $V_2$. These fingers can also form loops which transform into spherulites under an applied voltage larger than $V_2$, but not too high. These observations clearly show that the fingers are continuous, of the first type. More interesting is that these fingers drift perpendicularly to their axes and form spirals, particularly when one of their ends is attached to a dust particle (Figure 5). This result is not surprising at first

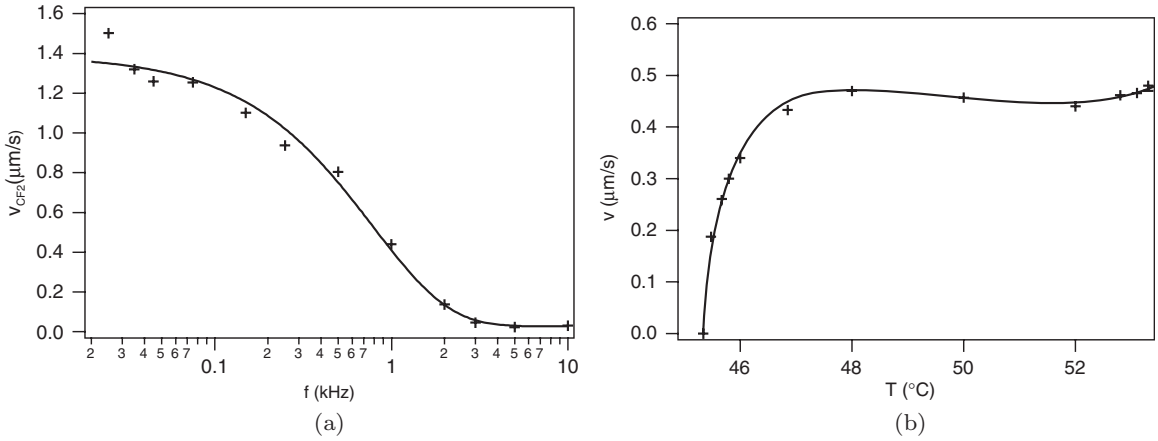


Figure 4. (a) Drift velocity of the CF2 as a function of frequency at $T = 52.3°C$. The solid line is the best fit to exponential function $v_0 \exp(-f/f_{CF2})$ with $f_{CF2} = 0.8$ kHz and $v_0 = 1.36\ \mu m\ s^{-1}$. (b) Drift velocity of the CF2 as a function of temperature at $f = 1$ kHz. Here $d = 15\ \mu m$. The solid line is just a guide for the eyes.

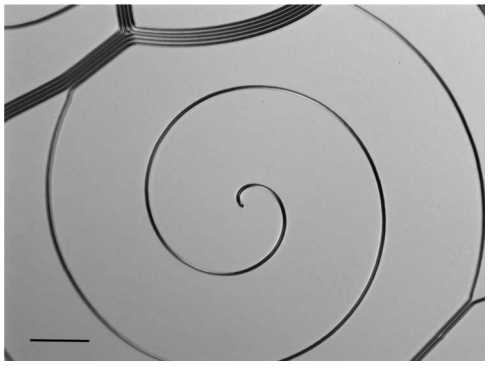

Figure 5. CF1 spiral observed in the coexistence region. Polariser and analyser are at 45° degrees relative to each other. The black scale bar is 100 μm long. Here $d = 15\ \mu m$, $\Delta T = 40°C$, $T = 54.5°C$, $f = 100$ Hz.



sight as we know from a previous work that CF1 can drift under the action of the temperature gradient (*23*).

On the other hand, we realised that in the present experiment the drift was essentially due to the electric field. This was clearly demonstrated by measuring $v_{CF1}$ as a function of frequency (Figure 6(a)). The fit of the data to the exponential function $v_0 \exp(-f/f_{CF1}) + v_\infty$ gives $f_{CF1} = 0.9$ kHz, $v_0 = 0.88\ \mu m\ s^{-1}$ and $v_\infty = 0.1\ \mu m\ s^{-1}$. This behaviour resembles that observed with the CF2, except that now a small drift is visible in the dielectric regime. This residual drift is clearly caused by the temperature gradient because it disappears when $\Delta T$ is decreased. We thus attribute it to the thermomechanical Lehmann effect associated with the temperature gradient (*23*). By contrast, the effect of the electric field in the conducting regime is more surprising because the CF1 do not drift ordinarily under an AC field. Nevertheless, it is important to note that this result is true only if the CF1 are invariant under a $\pi$-rotation about their long axes. This symmetry is obviously broken in our experiment because of the presence of the temperature gradient and the asymmetric boundary conditions (the anchoring is homeotropic on the cold plate and tilted at the interface with the isotropic liquid). As a consequence the drift of a CF1 under an AC field is no longer forbidden by symmetries and could be explained as well by using the same mechanisms as those used to explain the drift of the CF2. Finally, we measured $V_2$ and $v_{CF1}$ as a function of temperature in the coexistence region (Figure 6(b)). As expected, both quantities decrease when the temperature increases because the cholesteric layer becomes thinner.

### *4.3 CF1 spirals driven by the temperature gradient*

We did not observe any visible drift of the CF1 below the coexistence region, except close to the smectic phase. In this case, the CF1 spontaneously wind up around their rounded tips and form spirals (Figure 7(a)). After many hours the sample is invaded by spirals which pile up against each other (Figure 7(b)). It is worth noting that even in this final state the CF1 continue to drift, but not regularly because they must first break before they can be eliminated at the boundaries between spirals (Figure 7(b)). We measured the drift velocity of the free CF1 (i.e. before they touch each other) as a function of temperature at two different temperature gradients (Figure 8(a)). The same data are reported in Figure 8(b) as a function of the applied voltage, equal to (or slightly larger than) $V_2$. We see that the CF1 start to drift about 1°C above the transition temperature to the smectic phase. When the

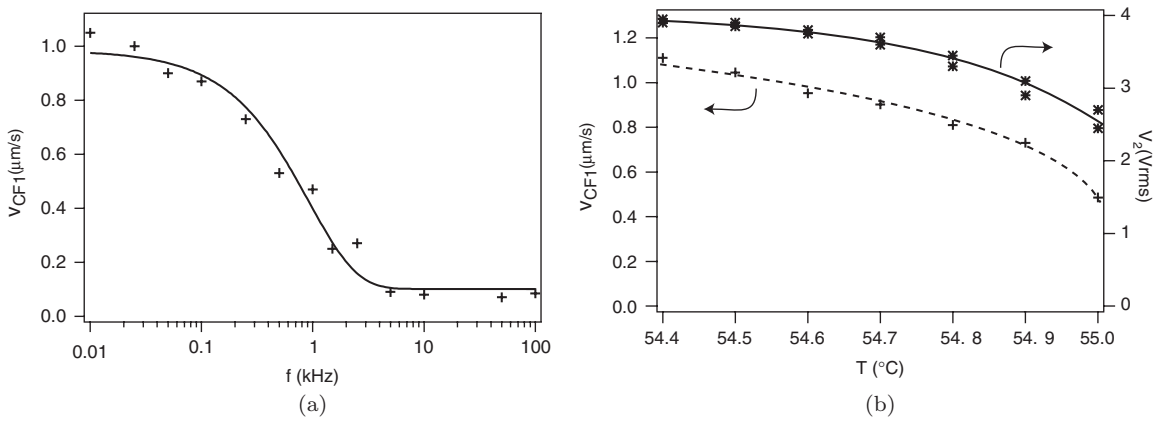


Figure 6. (a) Drift velocity of the CF1 as a function of frequency at $T = 55°C$. The solid line is the best fit to a single exponential function (see the text). (b) Drift velocity of the CF1 (left) and coexistence voltage (right) measured at $f = 1$ kHz as a function of temperature when the cholesteric phase coexists with the isotropic liquid. The solid and dashed lines are just guides for the eyes. Here $\Delta T = 40°C$ and $d = 15$ μm.

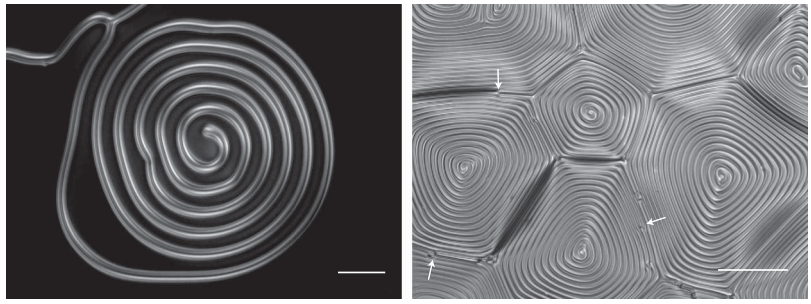


Figure 7. (a) Spiral formed from the rounded end of a CF1 close to the smectic phase. The white scale bar is 50 μm long. (b) Characteristic texture observed at long times. The arrows indicate places where the fingers are eliminated. The white scale bar is 100 μm long. The polariser and analyser are crossed. Here $T = 45.7°C$, $\Delta T = 40°C$, V = 1.98 V, $f = 1$ kHz and $d = 15$ μm.



temperature is decreased, their drift velocity first increases, then passes through a maximum and finally decreases until vanishing at the transition. We also found that the drift velocity was independent of the frequency of the electric field (Figure 9).

This last observation and the fact that $v_{CF1}$ decreases when $\Delta T$ is decreased (Figure 8) allow us to conclude that the drift is due to the temperature gradient.

The question that now arises is: why is the drift only observed in a small interval of temperature close to the transition? The fact that $v_{CF1}$ vanishes at the transition is certainly due to the divergence of the rotational viscosity $\gamma_1$ (the same effect was found for the drift of the CF2, see Figure 4(b)). By contrast, the vanishing of $v_{CF1}$ far from the transition is more surprising and could be due to the fact that the electric field inhibits the drift. Another unlikely possibility would be that the Lehmann coefficient increases when the transition to the smectic phase is approached. To find out which explanation is correct, we performed a similar experiment with the compensated mixture used in (*23*) (mixture of 8OCB and cholesteryl chloride in equal proportion by mass). In this mixture the Lehmann coefficient is finite at the compensation point and is a monotonic increasing function of temperature. We prepared a homeotropic 15 μm-thick sample of this mixture and measured the drift velocity of the CF1 as a function of voltage $V_2$, starting from the temperature at which $V_2 = 0$. Our results are given in Figure 10 and show very clearly that the electric field opposes the drift of the fingers.

This could explain why we only observe the thermal drift of the CF1 close to the smectic phase (Figure 8) and in the coexistence region (Figure 6) when $V_2$ is not too large.

## 5. Circular growth of the CF1

We have just seen that the CF1 stop drifting rapidly under the action of the temperature gradient when an electric field is applied. On the other hand, we observed that their growth from their two ends between $V_1$ and

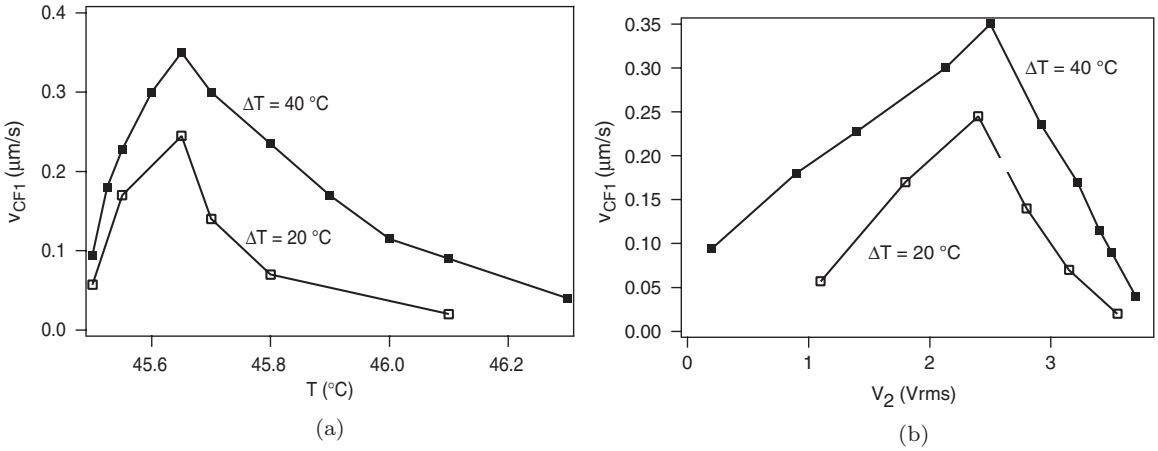


Figure 8. (a) Drift velocity of the CF1 as a function of temperature at two different temperature gradients. (b) Same data as a function of the applied voltage (equal to $V_2$). Here $\Delta T = 40°C$, $f = 1$ kHz and $d = 15$ μm.

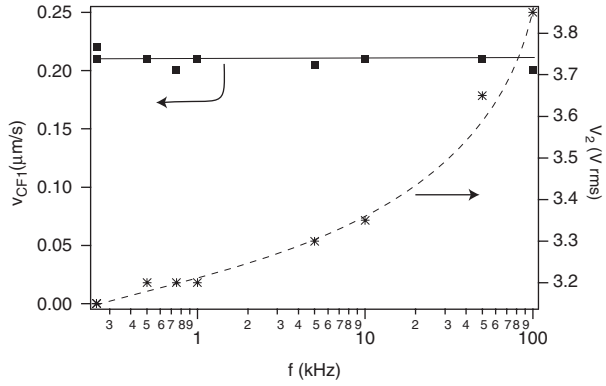


Figure 9. Drift velocity (left) and voltage $V_2$ (right) as a function of frequency. Note that $V_2$ is the voltage given by the function generator. Its increase at high frequency is essentially due to the finite resistance of the ITO electrodes (the voltage really seen by the sample is essentially constant as a function of frequency, of the order of 3.15 $V_{rms}$). Here $\Delta T = 40°C$, $T = 45.8°C$ and $d = 15$ μm.

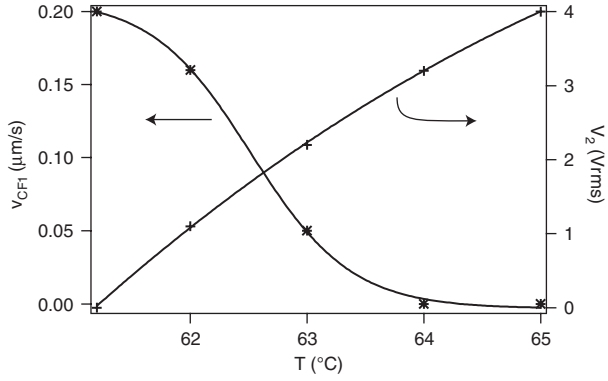


Figure 10. Velocity of the CF1 and coexistence voltage $V_2$ as a function of temperature above the compensation temperature. Instead of increasing when the temperature increases, the finger velocity decreases when an electric field is applied. Here $d = 15$ μm, $\Delta T = 30°C$.

$V_2$ was strongly modified by the temperature gradient. This is visible in Figure 11 where a finger growing from its rounded tip is shown. In Figure 11(a), there is no temperature gradient ($\Delta T = 0$) and the finger end propagates in straight line (*27*). This is normal because a CF1 is invariant by a $\pi$-rotation about its long axis (Figure 1(a)). In Figure 11(b) a temperature gradient is imposed ($\Delta T = 40°C$); now the finger tip grows to the left by following a circular trajectory. In Figure 11(c), the temperature gradient is of opposite sign ($\Delta T = -40°C$) and the finger grows this time to the right. A similar phenomenon is observed for the pointed tip, which also follows a circular trajectory when a temperature gradient is imposed (Figure 12). These observations are obviously permitted by symmetries because the rotation symmetry is broken by the presence of the temperature gradient. This point was stressed earlier by Frisch *et al.* (*28*) who also observed within a simplified two-dimensional numerical model the curvilinear growth of the finger tips in the presence of a DC electric field which is equivalent to a temperature gradient.

The trajectories of the two tips are characterised by their radii of curvature, $R_+$ for the rounded tip (+) and $R_-$ for the pointed tip ( – ). Note that $R_+$ and $R_-$ were found to be of opposite signs (with the convention that the finger is oriented from the pointed tip to the rounded tip, $R_+$ is positive and $R_-$ is negative in Figure 12). We measured curvatures $1/R_+$ and $1/R_-$ as a function of the applied voltage (Figure 13) and found that both quantities tend to finite values when the applied voltage tends to voltage $V_2$ at which the fingers stop growing. In the following we denote by

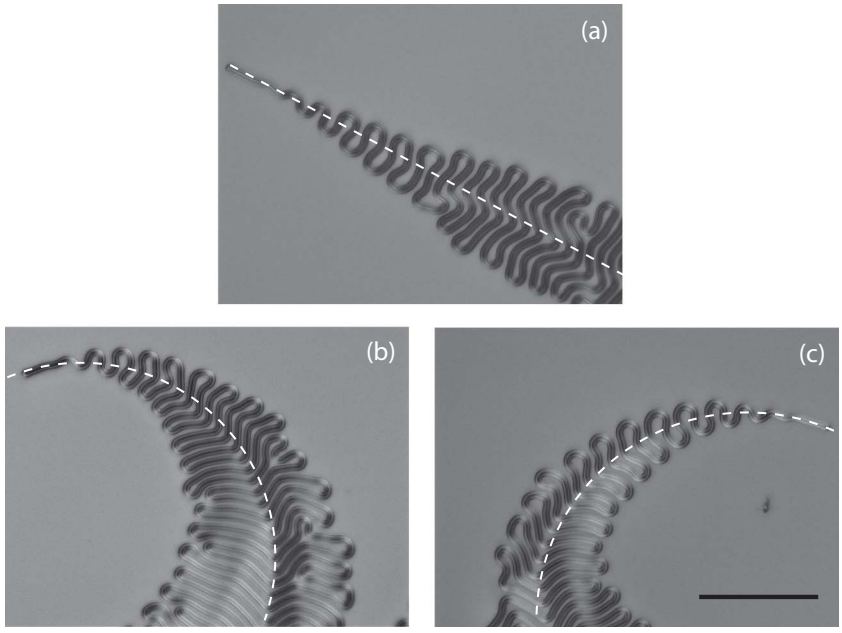


Figure 11. (a) Rectilinear growth in the absence of a temperature gradient ($\Delta T = 0°C$). (b), (c) Circular growth of a cholesteric finger when a temperature gradient is imposed: (b) $\Delta T = 40°C$ and (c) $\Delta T = -40°C$. The dotted lines (a straight line and two circles of the same radius in absolute value, respectively) show the trajectories followed by the rounded tip. The polariser and analyser are at 45° relative to each other. The black scale bar is 100 μm long. Here $d = 10$ μm, $T = 50°C$ and $V = 2\ V_{rms}$.



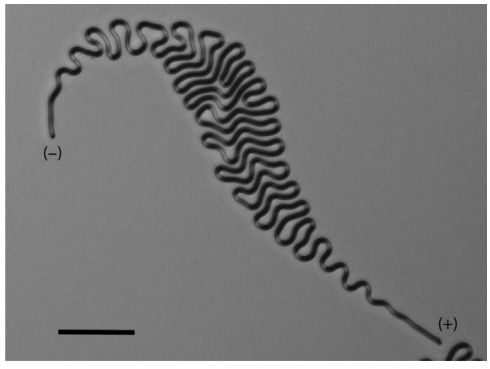


Figure 12. Growth of an isolated finger. Both tips are visible. The polariser and analyser are at 45° degrees relative to each other. The black scale bar is 100 μm long. Here $d = 10$ μm, $T = 48°C$, $\Delta T = 15°C$ and $V = 2\ V_{rms}$.

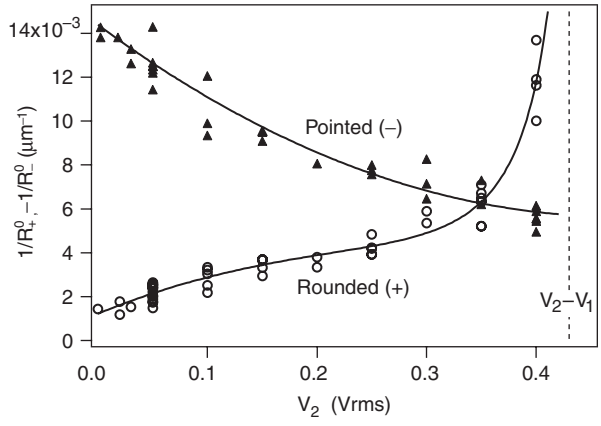


Figure 13. Curvatures as a function of the applied voltage when the latter is varied from $V_2$ down to $V_1$. Here $d = 10$ μm, $T = 48°C$ and $\Delta T = 40°C$.

$1/R^0_+$ and $1/R^0_-$ the curvatures measured in this quasi-static limit. These quantities are pertinent because they must be independent of the Leslie viscosities which are difficult to measure. For this reason, we focused our attention on them. We found that they are independent of the frequency (Figure 14) and linearly dependent on the temperature gradient (Figure 15). They also depend on the temperature and on the sample thickness as shown in Figure 16. In particular we see that, in absolute value, $1/R^0_+$ decreases and $1/R^0_-$ increases when the thickness increases.

The linear dependence of curvatures $1/R^0_+$ and $1/R^0_-$ on the temperature gradient and their independence to frequency suggest that the Lehmann torque, of the expression (*29*)

$$\Gamma_{\text{Lehm}} = \nu \boldsymbol{n} \times (\boldsymbol{n} \times \boldsymbol{G}) \qquad (1)$$

where $\nu$ is the Lehmann coefficient, is responsible for the circular growth of the fingers. Note that there are several lengths in this problem: the sample thickness $d$, the cholesteric pitch $p$ and at least three thermal

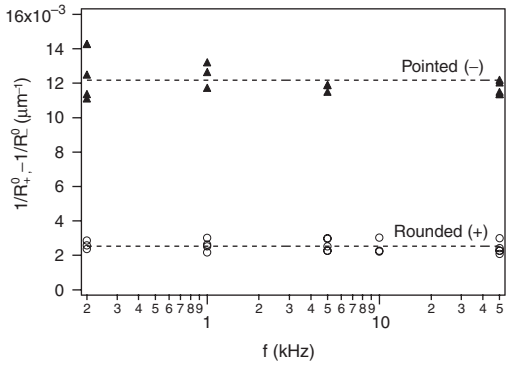


Figure 14. Curvatures as a function of frequency in the quasi-static limit (at $V = V_2$). Here $d = 10$ μm, $T = 48°C$ and $\Delta T = 40°C$.

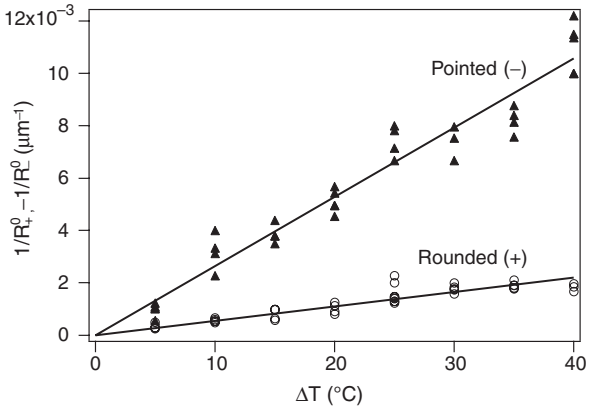


Figure 15. Curvatures as a function of temperature gradient in the quasi-static limit (at $V = V_2$). Here $d = 10$ μm, $T = 48°C$ and $f = 1$ kHz.

lengths of the type $\sqrt{K_i/\nu G}$ where $K_i$ ($i = 1, 2, 3$) are the Frank elastic constants (and, by neglecting the temperature variation of the elastic constants and of the pitch, this is certainly wrong close to the smectic phase). It is thus impossible from dimensional arguments to predict how curvatures scale with the problem parameters and only a full numerical resolution of the torque equation in the quasi-static limit could allow one to predict the corresponding curvatures as a function of the Lehmann coefficient.

## 6. Conclusions

We have studied the behaviour of cholesteric fingers subjected to the combined action of an AC electric field and a temperature gradient.

We have found, in agreement with previous studies (*20*), that the CF2 drift and form spirals under AC electric field in the conducting regime and stop drifting in the dielectric regime. In contrast, we did not observe

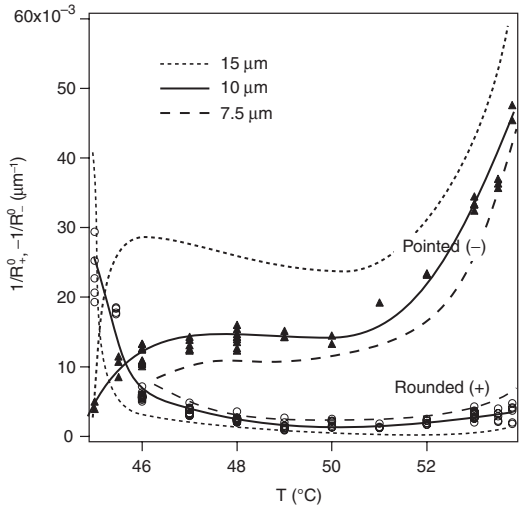


Figure 16. Curvatures as a function of temperature in the quasi-static limit (at $V = V_2$). Solid line: $d = 10$ μm; dashed line: $d = 7.5$ μm; dotted line: $d = 15$ μm. For clarity, only the experimental points corresponding to $d = 10$ μm have been reported. Here $T = 48°C$ and $f = 1$ kHz.

any visible drift of the CF2 mediated by the temperature gradient. As the CF2 are difficult to produce, we paid more attention to the CF1 which spontaneously nucleate at low voltages. We found that the CF1 only drift under special conditions, in particular close to the smectic phase, when the electric field is not too large. In this case, the drift velocity is unchanged at all frequencies and vanishes when the temperature gradient is removed. This clearly suggests that the drift is due here to the thermal Lehmann effect. The fact that the drift disappears when the temperature tends to the transition temperature to the smectic phase is probably due to the divergence of the rotational viscosity. We also observed the drift of the CF1 in the coexistence region with the isotropic liquid, when the cholesteric phase forms an asymmetric layer in contact with the electrode on one side and with the isotropic liquid on the other side. Under these conditions, we observed that the drift was mainly due to the electric field with a small contribution coming from the temperature gradient. This effect of the electric field is not forbidden because the rotation symmetry of the CF1 is broken by the temperature gradient and the presence of different anchoring conditions on the two bounding surfaces. Finally, we found that the AC electric field inhibits the drift of the CF1 under usual conditions. This unexpected point was checked by using the compensated mixture studied before and remains to be explained theoretically.

We then described the circular growth of the fingers. This phenomenon, which has been already observed in the numerical simulations of Frisch *et al.* (*28*), was

clearly identified as due to the temperature gradient and the thermal Lehmann effect. It could thus be used to measure the Lehmann coefficient but this requires us to solve the torque equation numerically for the director field at three dimensions in the quasi-static limit. This has already been done at constant temperature without electric field by Nagaya *et al.* (*30*). Extending such calculations in the presence of an AC electric field and a temperature gradient provides an interesting challenge for theorists in the future.

## References


(1) Oswald, P.; Pieranski, P. *Nematic and Cholesteric Liquid Crystals: Concepts and Physical Properties Illustrated by Experiments*; Taylor & Francis: Boca Raton, FL, 2005; Chapter B.VII.
(2) Oswald, P.; Baudry J.; Pirkl, S. *Phys. Rep.* **2000**, *337*, 67–96.
(3) Baudry, J.; Pirkl, S.; Oswald, P. *Phys. Rev. E* **1998**, *57*, 3038–3049.
(4) Press, M.J.; Arrott A.S. *J. Phys. (Paris)* **1976**, *37*, 387–395.
(5) Gil, L.; Gilli, J.M. *Phys. Rev. Lett.* **1998**, *80*, 5742–5745.
(6) Baudry, J.; Pirkl, S.; Oswald, P. *Phys. Rev. E* **1999**, *59*, 5562–5571.
(7) Smalyukh, I.I.; Senyuk, B.I.; Palffy-Muhoray, P.; Lavrentovich, O.D.; Huang, H.; Gartland, E.C., Jr.; Bodnar, V.H.; Kosa, T.; Taheri, B. *Phys. Rev. E* **2005**, *72*, 061707.
(8) Oswald, P.; Dequidt A. *Phys. Rev. Lett.* **2008**, *100*, 217802.
(9) Oswald, P. *Eur. Phys. J. E* **2009**, *28*, 377–383.
(10) Éber, N.; Jánossy, I. *Mol. Cryst. Liq. Cryst. Lett.* **1982**, *72*, 233–238.
(11) Éber, N.; Jánossy, I. *Mol. Cryst. Liq. Cryst. Lett.* **1984**, *102*, 311–316.
(12) Dequidt, A.; Żywociński, A.; Oswald, P. *Eur. Phys. J. E* **2008**, *25*, 277–289.
(13) Oswald, P.; Dequidt, A. *EPL* **2008**, *83*, 16005.
(14) Delenclos, S.; Kolinsky, C.; Longuemart, S.; Hadj Sahraoui, A.; Buisine, J.M. *J. Therm. Anal. Cal.* **2002**, *70*, 549–558.
(15) Gilli, J.M.; Kamayé, M. *Liq. Cryst.* **1992**, *11*, 791–796.
(16) Mitov, M.; Sixou, P. *J. Phys. II (France)* **1992**, *2*, 1659–1670.
(17) Mitov, M.; Sixou, P. *Mol. Cryst. Liq. Cryst.* **1993**, *231*, 11–28.
(18) Ribière, P.; Oswald, P.; Pirkl, S. *J. Phys. II (France)* **1994**, *4*, 127–143.
(19) Pirkl, S.; Oswald, P. *J. Phys. II (France)* **1996**, *6*, 355–373.
(20) Baudry, J.; Pirkl, S.; Oswald, P. *Phys. Rev. E* **1999**, *60*, 2990–2993.
(21) Pirkl, S.; Oswald, P. *Liq. Cryst.* **2001**, *28*, 299–306.
(22) Tarasov, O.S.; Krekhov, A.P.; Kramer, L. *Phys. Rev. E* **2003**, *68*, 031708.
(23) Oswald, P.; Dequidt, A. *Phys. Rev. E* **2008**, *77*, 051706.
(24) Brochard, F. *J. Phys. Paris* **1973**, *34*, 411–422.
(25) DasGupta, S.; Roy, S.K. *Phys. Lett. A* **2003**, *306*, 235–242.
(26) Faetti, S.; Palleschi, V. *Phys. Rev. A* **1984**, *30*, 3241–3251.
(27) Nagaya, T.; Hikita, Y.; Orihara, H.; Ishibashi, Y. *J. Phys. Soc. Japan* **1996**, *65*, 2707–2712.
(28) Frisch, T.; Gil, L.; Gilli, J.M. *Phys. Rev. E* **1993**, *48*, R4199–R4202.
(29) Leslie, F.M. *Proc. R. Soc. A* **1968**, *307*, 359–372.
(30) Nagaya, T.; Hikita, Y.; Orihara, H.; Ishibashi, Y. *J. Phys. Soc. Japan* **1996**, *65*, 2713–2716.